



## Research article

# Biogenic mediated green synthesis of NiO nanoparticles for adsorptive removal of lead from aqueous solution

Abdurohman Eshtu Ferenji<sup>a</sup>, Yeshe Endris Hassen<sup>a</sup>, Shewaye Lakew Mekuria<sup>b</sup>,  
Wubshet Mekonnen Girma<sup>a,\*</sup>

<sup>a</sup> Department of Chemistry, College of Natural Science, Wollo University, P.O. Box:1145, Dessie, Ethiopia

<sup>b</sup> Department of Chemistry, College of Natural and Computational Sciences, University of Gondar, Gondar, 196, Ethiopia

## ARTICLE INFO

## Keywords:

Adsorption

NiO NPs

*Hagenia abyssinica*

Heavy metals

Green synthesis

## ABSTRACT

The spread of heavy metal in water bodies, particularly lead (Pb), has occurred as a global threat to human existence. In this study, NiO nanoparticles (NPs) was prepared by coprecipitation approach using *Hagenia abyssinica* plant extract mediated as a reducing and template agent for the removal of Pb from aqueous solution. X-ray crystallographic diffraction (XRD), Scanning electron microscopy (SEM), Fourier transform infrared (FTIR), and Brunauer-Emmett-Teller (BET) techniques were employed for the characterization of as prepared NiO NPs. The efficacy of adsorbent was evaluated on the removal of Pb<sup>2+</sup> by varying the adsorptive parameters such as pH, Bio-NiO amount, interaction time, and Pb<sup>2+</sup> concentration. The adsorption was 99.99% at pH, 0.06 g of NiO NPs dose, 60 mg L<sup>-1</sup> concentrations of Pb<sup>2+</sup> within 80 min contact time. The higher removal efficiency is could be due to higher surface area (151 m<sup>2</sup>g<sup>-1</sup>). The adsorption process was best fitted with Freundlich isotherm and pseudo-second order kinetic models, implying that it was chemical adsorption on the heterogeneous surface. The adsorption intensity (n) was found to be 1/n < 1 (0.47) indicating adsorption of Pb<sup>2+</sup> on the surface of Bio-NiO NPs was favorable with a maximum adsorption capacity 60.13 mg g<sup>-1</sup>. The reusability studies confirmed that the synthesized bio-NiO NPs were an effective adsorbent for removing Pb<sup>2+</sup> from aqueous solution up to five cycles.

## 1. Introduction

Increased demand for global resources is a result of industrialization and urbanization caused by the expanding human population [1]. This leads to an exponential increase in the amount of waste generated by various industrial activities. Some of industrial activities like electroplating, ore mining, refining, tanning, dyeing, and tire manufacturing all increase the use of heavy metals, including Cd, Pb, Hg, and Cr [2]. The life processes of biota are significantly impacted when these heavy metals are released into water bodies without proper treatment [3]. Owing to its nonbiodegradable nature their presence in water, even at low concentrations, is hazardous to both human health and aquatic life [4]. Pb and its compounds are a versatile and strategically significant metal for industrial development since they are intricately tied to the automotive industry, power generation, energy storage, mining, refining, acid industries, smelting, battery production, and other industries [1,5]. The widespread use of Pb<sup>2+</sup> ions causes significant water contamination, which eventually accumulates via the food chain. Pb is a metal that is both mutagenic and teratogenic, with toxic effects on the immune

\* Corresponding author.

E-mail address: [wubshet.mekonnen@wu.edu.et](mailto:wubshet.mekonnen@wu.edu.et) (W.M. Girma).

<https://doi.org/10.1016/j.heliyon.2024.e31669>

Received 22 February 2024; Received in revised form 18 May 2024; Accepted 20 May 2024

Available online 22 May 2024

2405-8440/© 2024 The Authors. Published by Elsevier Ltd. This is an open access article under the CC BY-NC-ND license (<http://creativecommons.org/licenses/by-nc-nd/4.0/>).

system, bone marrow, neurological system, and kidney, especially in young children [6].  $\text{Pb}^{2+}$  exists in both organic and inorganic forms, and the physicochemical makeup of the exposed individual has a significant impact on how quickly it is absorbed by humans. Inorganic Pb cannot be digested, it spreads and accumulates in soft tissues and bones without being directly ejected, but organic Pb found in gasoline can be absorbed through the skin and respiratory system. Pb is indicated as a priority, with a concentration of less than  $0.01 \text{ mgL}^{-1}$  in drinking water according to WHO regulations [5].

Various methods, including membrane or ultra-filtration [7], co-precipitation [8], electro coagulation [9], reverse osmosis [10], ion exchange [11], and adsorption [12,13] are used to remove heavy metals from water. However, some of these processes have some downsides, including sensitive operation, high energy requirements, the formation of hazardous sludge, and a lack of adequate waste disposal, which limits their efficiency [14]. Among these techniques, adsorption is thought to be an effective technique than other techniques due to its high efficacy, cheap execution costs, sufficient accessibility, and straightforward design and easy regeneration of the adsorbents [15]. The adsorption process relies on the physicochemical features of heavy metals and adsorbents, as well as operational variables like pH, adsorbent quantity, temperature, adsorption period, and initial metal ion concentration [16,17]. So far a variety of conventional adsorbents such as natural zeolites, activated charcoal, and synthetic resins are employed to extract pollutants from industrial effluent with some restrictions [18]. However, these adsorbents showed a low adsorption performance as compared to nanostructure crystalline metal oxides. In recent years, metal oxide nanoparticles (NPs) have gained significant attention in the adsorption process due to their large surface area, adsorptive nature, surface flaws, and fast diffusivities [19]. These features make them effective adsorbent material for removal of heavy metals from water. Among metal oxide, NiO NPs offer an appropriate adsorption capability for the removal of heavy metals from waste water due to their high surface area, low production cost, and natural porosity [20,21]. Benefiting from the discovery of nanotechnology, synthesis of NPs using a greener approach with a superior performance became a popular research in wastewater treatment. Until now traditional chemical synthesis routes were widely employed for the synthesis of NiO NPs which have health and safety related issues. Moreover, using toxic chemicals like acids and bases for the synthesis of NPs have its own toxic effects [22]. In this regard, bio-derived materials offer an alternative to environmentally friendly supports. Biological approaches offer the following advantages over other methods [23–25]: (i) There is no need for expensive, hazardous stabilizers or capping agents; (ii) the final product does not need to be processed at high temperatures; (iii) no hazardous ingredients or dangerous organic solvents are required; and (iv) the procedures are easy to scale up. Recent studies indicate that plant extract stabilized NPs and nanocomposites were applied for remediation of contaminated water and showed greater progress for the use of plant extracts for reducing metal oxide precursors as well as capping the NPs [26–28]. Because it includes a large number of potentially active phytochemicals that are crucial to the stability or reduction of metal salts throughout the synthesis process, it is chosen for the green synthesis of NPs [29]. To avoid aggregation, control particle size, and promote surface functionalization, plant extract was employed as a template and capping agent. Among renewable natural resources, *Hagenia abyssinica* is a medicinal plant that can be used as a template to build nanoparticle-based adsorbents for wastewater treatment. Owing to the presence of biomolecules in *Hagenia abyssinica* such as saponins, phenolbathanins, flavonoids, anthraquinones, phenols, terpenoids, alkaloids, steroids, glycosides, and tannins we have selected as a reducing and capping agent for the synthesis of NiO NPs [30].

Considering the natural abundance, its low production cost, higher surface area, herein we report *Hagenia abyssinica* biomediated synthesis NiO NPs for removal of lead from aqueous solution. The synthesis of NiO NPs was carried out using  $\text{Ni}(\text{NO}_3)_2 \cdot 6\text{H}_2\text{O}$  in aqueous media. *Hagenia abyssinica* plant as a reducing agent and capping/stabilizer to control the particle size during NiO NPs synthesis, making it novel and innovative. The as prepared NPs were characterized using x-ray diffraction (XRD), scanning electron microscopy (SEM), Fourier transform infrared (FTIR), and Brunauer-Emmett-Teller (BET). For comparison purpose we have used chemical synthesis route to create NiO NPs as a control experiment. The generated NPs were tested for removal of  $\text{Pb}^{2+}$  from aqueous solution, showed outstanding removal performance (99.99%). It is predicted that the increased removal efficiency is due to the larger surface area ( $151 \text{ m}^2\text{g}^{-1}$ ), which is a feature of mesoporous adsorbents with poor adsorbate-adsorbent interaction at low relative pressure. Furthermore, to better understand the adsorption process, we investigated adsorption isotherms using the most used models and estimated adsorption kinetics.

## 2. Materials and methods

### 2.1. Chemicals and reagents

All chemicals and reagents used in this study were analytical grades. Nickel nitrate hexahydrate ( $\text{Ni}(\text{NO}_3)_2 \cdot 6\text{H}_2\text{O}$  MW = 290.81 g/mol, SAMIR.TECH-CHEM, 98%), extra pure Ammonia ( $\text{NH}_3$ , MW = 17 g/mol, 25%), Sodium hydroxide (NaOH, MW = 39.999 g/mol, Norbright, turkey, 99%), and Ethanol ( $\text{CH}_3\text{CH}_2\text{OH}$ , MW = 46.07 g/mol, 99.9%). All the aqueous solutions were prepared by using double distilled water throughout the experiments. To create the stock solution of  $\text{Pb}^{2+}$ , lead nitrate ( $\text{Pb}(\text{NO}_3)_2$  MW = 331.2 g/mol, 99%) was dissolved in distilled water. Furthermore, to alter the pH of solutions, HCl (0.1 N, MW = 36.458 g/mol) was utilized.

### 2.2. Preparation of *Hagenia abyssinica* plant extract

*Hagenia abyssinica* leaves were collected from Dessie campus, Wollo University. Tap water and deionized water was used to wash dust particles, followed by drying at ambient temperature. Then, it was powdered using electric grinder. 20 g powder was transferred to an Erlenmeyer flask containing 400 mL of distilled water. Afterward, the mixture was mechanically shaken for 30 min followed by stirring for 1 h  $50^\circ\text{C}$ . Subsequently, after cooling to ambient temperature the solution was purified using whatman No.1 filter paper. Finally, the filtrate was kept at  $4^\circ\text{C}$  for subsequent use [31].

## 2.3. Preparation of nickel oxide (NiO) nanoparticles (NPs)

### 2.3.1. Chemical synthesis of NiO NPs

NiO NPs were produced by dissolving 0.3 M Ni(NO<sub>3</sub>)<sub>2</sub>•6H<sub>2</sub>O salt in 100 mL of distilled water and stirring for 30 min. A 100 mL solution of 1.3 M NaOH was slowly added to the aforementioned solution and agitated at 70 °C for 2 h. The resulting greenish gel was allowed to cool to ambient temperature. Subsequently, it was washed several times with water and ethanol to remove contaminants, followed by drying at 80 °C. The product was calcined in a muffle furnace at 400 °C for 2 h, resulting in black NiO powder (labeled as Chem-NiO NPs).

### 2.3.2. *Hagenia abyssinica* plant extract biomediated synthesis of NiO NPs

To the aqueous solution of 0.05 M (NO<sub>3</sub>)<sub>2</sub>•6H<sub>2</sub>O in 50.0 mL 2 M NH<sub>3</sub> solution was added to adjust the pH to 11, followed by gentle stirring until it changed to dark blue at 80 °C, indicating the formation of [Ni(NH<sub>3</sub>)<sub>6</sub>] complex. Subsequently, 50.0 mL of *Hagenia abyssinica* plant extract was dropwise added and stirred for additional 90 min. The light-green product was allowed to cool to ambient temperature. After washing with deionized water and ethanol it was allowed to dry in oven at 100 °C for overnight. Finally, the greyish black NiO NPs (labeled as Bio-NiO NPs) were obtained via calcination of Ni(OH)<sub>2</sub> powder at temperature of 300 °C in a muffle furnace for 2 h.

## 2.4. Characterization

To characterize the crystallites of NiO NPs x-ray diffraction (XRD) peaks were obtained using Shimadzu XRD-7000. The surface morphology of the NiO NPs were obtained by using field-emission scanning electron microscopy (FESEM, JSM 6500F, JEOL). The surface functional groups of the NiO NPs were studied using Fourier transform infrared (FT-IR) spectra by using 65 FT-IR (PerkinElmer) spectroscopy. Nitrogen adsorption measurements were carried out on the 3-Flex Surface Characterization Analyzer (Mercurius) with guest-free (evacuated) samples at pressures up to 1 bar. The surface areas were estimated using the Brunauer-Emmett-Teller (BET) model from nitrogen adsorption isotherms collected at 77 K. Pore size distribution was analyzed using a BJH model from the desorption branch. The DW-AA320 N Atomic Absorption spectrometer (AAS) was used for adsorption studies. Surface potentials were conducted using the Zeta sizer Pro BLUE equipment from Malvern, UK. The electrophoretic mobility of particles was automatically calculated and then converted to zeta potential using the Smoluchowski equation (Equation (1)).

$$\zeta = (\eta \times \mu) / \epsilon \quad (1)$$

Where,  $\zeta$  is the zeta potential,  $\eta$  is the dynamic viscosity,  $\mu$  is the particle mobility, and  $\epsilon$  is the dielectric constant. 0.1 g of NiO NPs were dissolved in 100 mL of deionized water under stirring for 15 min, resulting in a 0.1 % solid ratio. The solutions pH was adjusted using 0.1 M HCl and 0.1 M NaOH. Subsequently, the solution was allowed to undisturbed for 30 min to settle larger particles.

## 2.5. Batch adsorption experiments

Adsorption study was conducted in a batch method for removal of Pb<sup>2+</sup> ion using Bio-NiO NPs. By varying experimental parameters including pH value, the adsorbent dose, contact time, and initial Pb<sup>2+</sup> concentration the optimal adsorption conditions of Bio-NiO NPs were studied. All tests were performed at room temperature. A stock solution of Pb<sup>2+</sup> (1000 mg L<sup>-1</sup>) was prepared by dissolving the calculated quantity of Pb(NO<sub>3</sub>)<sub>2</sub> for Pb<sup>2+</sup> in deionized water. The effect of solution pH on the removal of metal ion were performed in range from 3 to 12 and during the experiment the solution acidity was adjusted by dropping 0.1 M HCl and 0.1 M NaOH solutions. 40–100 min were used to demonstrate the effects of contact time. The effect of adsorbent dose and Pb<sup>2+</sup> ion concentrations were conducted at various amount as 0.03–0.12 g and concentration from 40 to 100 mg L<sup>-1</sup>, respectively. The solutions were shaken by shaker at 200 rpm until the adsorption process reached equilibrium, supernatant liquid was separated by using whatman filter paper and it is used for analysis of adsorbed Pb<sup>2+</sup> ion using AAS. The metal ion removal efficiency (%R) and the concentration of adsorbate which adsorbed at equilibrium, q<sub>e</sub> (mg/g) were calculated by Equation (2) and Equation (3), respectively.

$$\%R = \frac{(C_0 - C_e)}{C_0} \times 100 \quad (2)$$

$$Q_e = \frac{(C_0 - C_e)}{W} \times V \quad (3)$$

Where, Q<sub>e</sub> is the concentration of Pb<sup>2+</sup> ions adsorbed on Bio-NiO NPs at equilibrium, %R is percent removal, V is the volume of a solution in L, W is the weight of Bio-NiO NPs in gram scale, and C<sub>0</sub> and C<sub>e</sub> are the initial and equilibrium concentrations (mg L<sup>-1</sup>), respectively.

## 2.6. Recovery studies

To conduct desorption tests, metal-adsorbed Bio-NiO NPs were rinsed with ultrapure water to eliminate any loosely attached metals from the vial and adsorbent. HCl was used to desorb Pb ions, with eluent concentrations ranging from 0.001 to 0.2 M. To investigate

recovery, five successive cycles of Bio-NiO NPs regeneration and metal re-adsorption were performed. In each cycle, 0.06 g Bio-NiO NPs were mixed with 60 mL of  $100 \text{ mg L}^{-1} \text{ Pb}^{2+}$  ion. In each cycle, the Bio-NiO NPs were washed with deionized water to attain neutral condition and adjusted for removal of  $\text{Pb}^{2+}$  in the next cycle. The Bio-NiO NPs were filtered and supernatant were used to calculate the amount of  $\text{Pb}^{2+}$  adsorbed. All measurements were conducted in triplicate.

### 3. Results and discussion

#### 3.1. Synthesis and characterization

The fabrication of the Chem-NiO NPs was carried out by using aqueous solutions of  $\text{Ni}(\text{NO}_3)_2 \cdot 6\text{H}_2\text{O}$  and NaOH. However, synthesis of Bio-NiO NPs were employed using a *Hagenia abyssinica* leaf extract (Scheme 1). In a clear solutions of  $\text{Ni}(\text{NO}_3)_2 \cdot 6\text{H}_2\text{O}$  pH was adjusted to 11 by adding  $\text{NH}_3$  and allowed to heat for  $80^\circ \text{C}$  followed by formation of an intermediate dark blue complex. Afterward, the plant extract added and allowed to reduce the metal salt and stabilize the NPs and a light-green precipitate product was dried and calcined to obtain Bio-NiO NPs.

The phase purity and crystallites of NiO NPs were assessed by using XRD (Fig. 1). For Chem-NiO NPs the peaks appeared at  $2\theta = 29.5705^\circ, 37.4558^\circ, 43.5013^\circ, 63.0887^\circ, 75.6087^\circ, \text{ and } 79.5587^\circ$ . For Bio-NiO NPs the peaks are positioned at an angle of  $2\theta = 37.2661^\circ, 43.3147^\circ, 62.8827^\circ, 75.4085^\circ, \text{ and } 79.3722^\circ$ , which are corresponding to the (111), (200), (220), (311), and (222) plane of the cubic structure for both synthesized NiO NPs, respectively [32]. However, the peak appeared at  $2\theta = 29.5705^\circ$ , for Chem-NiO NPs, its indexed (110) [22]. The diffraction peaks of the NPs matched with the JCPDS, No. 04–0835. The obtained spectra indicate that the prepared NiO NPs have well crystalline nature. The average particle size of Chem/Bio-NiO NPs were evaluated from the width of the peaks using Debye-Scherrer's formula [33] by taking the three strongest peaks of Chem-NiO at  $2\theta = 29.5705^\circ, 37.4558^\circ, 43.5013^\circ$ , and Bio-NiO NPs at  $2\theta = 37.2661^\circ, 43.3147^\circ, 62.8827^\circ$ . Therefore, particle sizes were found to be for Chem-NiO and Bio-NiO NPs is 15.89 nm and 11.83 nm, respectively.

FT-IR characterization was also performed to support the formation of the synthesized nanoadsorbent (NiO NPs) (Fig. 2). The FT-IR spectrashowed that significant absorption peaks appeared around  $3353 \text{ cm}^{-1}$  and  $3471 \text{ cm}^{-1}$  attributed to the O–H stretching vibrations of interlayer water molecules for Chem-NiO and Bio-NiO NPs, respectively. The peaks from  $1394$  to  $1616 \text{ cm}^{-1}$  &  $1380$ – $1699 \text{ cm}^{-1}$  are assigned to H–O–H bending mode of the water molecule of both Chem-NiO and Bio-NiO NPs, respectively [34]. The C–O stretching vibrations are appeared at  $1018 \text{ cm}^{-1}$  and  $1100 \text{ cm}^{-1}$  for Chem-NiO and Bio-NiO NPs, respectively [32,35]. The strong band at  $448 \text{ cm}^{-1}$  and  $429 \text{ cm}^{-1}$  assigned to the Ni–O stretching for Chem- and Bio-NiO NPs, respectively [36].

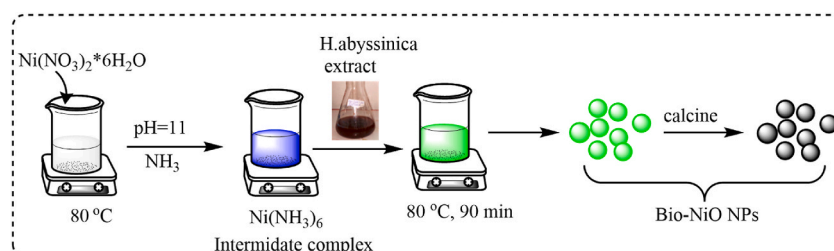
The morphologies of as prepared Bio-NiO NPs were analyzed using SEM. As shown in the SEM image of Bio-NiO NPs in Fig. 3a, agglomerated and very thin linked nature of particles with nanosheet microstructure was dominant. Fig. 3b revealed that the existence of Ni and O from its corresponding EDX of Bio-NiO NPs. The corresponding percentage in weight and atomic for Ni (83.70 % and 58.32 %) and for oxygen (16.30 % and 41.65 %), revealed that NiO nanoadsorbent was successfully formed.

For adsorption of pollutants surface area and pore size distribution of the adsorbent material could affect the adsorption capacity [37].  $\text{N}_2$  adsorption experiment was conducted at 77 K to determine the specific surface area and porosity of NPs. Prior to the  $\text{N}_2$  adsorption testing, about 200 mg of the as-synthesized compounds were evacuated/activated by heating them under a dynamic vacuum at  $150^\circ \text{C}$  for 8 h. The  $\text{N}_2$  adsorption isotherms recorded at 77 K (Fig. 4) revealed that the pure Bio-NiO NPs exhibited a type-IV isotherm, a mesoporous material according to the International Union of Pure and Applied Chemistry (IUPAC) classification [38], with BET surface areas of approximately  $151 \text{ m}^2 \text{ g}^{-1}$  and low hysteresis at high relative pressures. This trait is also shared by mesoporous adsorbents, which have weak adsorbate-adsorbent interactions at low relative pressure. The textural properties of produced NPs, such as a particular surface area, pore size, and pore volume distribution, are critical for adsorption applications. As a result, highly porous Bio-NiO NPs with high BET surface area makes a good adsorbent for removal application. The pore-size distribution was estimated using the BJH approach based on the desorption branch of the isotherm. The hysteresis loop was observed in the relative pressure range of 0.45–0.98, indicating mesoporous Bio-NiO NPs [39].

#### 3.2. Adsorption studies

##### 3.2.1. Effect of initial pH

The effect of pH on the adsorption of  $\text{Pb}^{2+}$  onto Bio-NiO NPs was tested at various pH range of 3–12 with other parameters holding



Scheme 1. Schematic representations of *Hagenia abyssinica* plant extract mediated synthesis of NiO NPs.

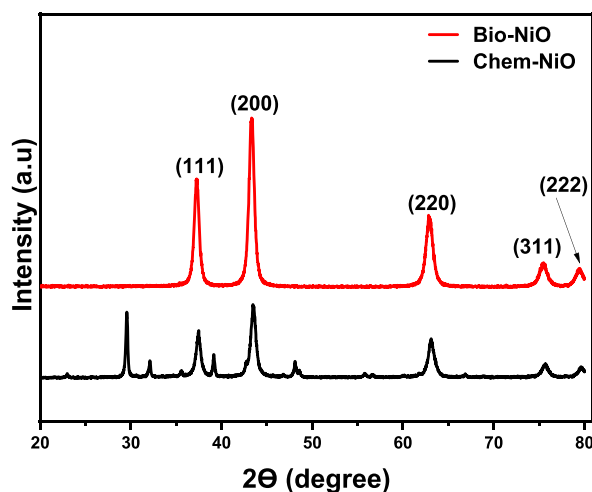


Fig. 1. The XRD patterns for as synthesized Chem-NiO and Bio-NiO NPs.

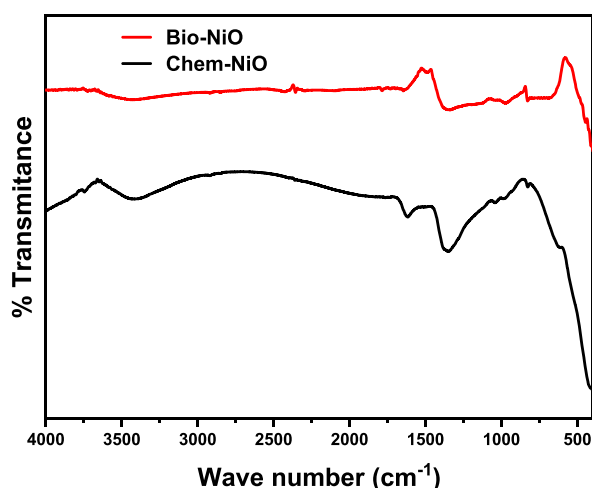


Fig. 2. FT-IR spectra of as synthesized Chem-NiO and Bio-NiO NPs.

constant i.e. adsorbent dose 0.06 g, initial  $\text{Pb}^{2+}$  ion concentration  $60 \text{ mgL}^{-1}$  and 80 min contact time (Fig. 5a). Because pH influences both the degree of adsorbent ionization and the solubility of the metal ion, it has a considerable impact on the  $\text{Pb}^{2+}$  adsorption mechanism onto Bio-NiO NPs. Thus, adsorption should be carried out at the optimal pH. At lower pH 3 the removal efficiency was 79.51%. However, by increasing the pH value from 6 to 12 the removal efficiency goes towards higher values and achieves a maximum of 99.99% at pH 6.0. Further increase in pH results in precipitation of  $\text{Pb}^{2+}$  as  $\text{Pb}(\text{OH})_2$  [40]. The findings are thus accurately explained by surface complex formation theory, which states that at low pH, in the acidic zone  $\text{pH} < 6$ , the removal efficiency was low due to the presence of  $\text{H}^+$  and  $\text{Pb}^{2+}$  species, which compete for the same binding site and reduce the proportion of metal ion adsorption. However, at higher pH levels, the surface of Bio-NiO becomes negatively charged, favoring interactions with  $\text{Pb}^{2+}$  ions and therefore increasing  $\text{Pb}^{2+}$  removal %. At pH 7–12, different species of  $\text{Pb}^{2+}$ , such as  $\text{Pb}(\text{OH})^+$  and  $\text{Pb}(\text{OH})_2$ , become prominent, resulting in increased removal efficiency by adsorption of  $\text{Pb}(\text{OH})^+$  and precipitation of  $\text{Pb}(\text{OH})_2$  concurrently [41,42].

To demonstrate the interaction between Bio-NiO NPs and  $\text{Pb}^{2+}$ , surface potentials of the Bio-NiO was carried out at across varying pH values. Zeta potential ( $\zeta$ ) value tend to increase to negative value with increasing pH 6 while it slightly decreased as the pH increased (Fig. 5b). This tends to increase the interaction between Bio-NiO NPs and  $\text{Pb}^{2+}$  at negative surfaces tend to increase adsorption of  $\text{Pb}^{2+}$  on the adsorbent. At lower pH value the deprotonation of functional groups (could be O–H and COOH) is slightly limited. However, as the pH climbed to 6, the surface of NPs became negatively charged ( $\zeta = -18 \text{ mV}$ ), facilitating the deprotonation of surface functional groups and metal adsorption. The possible adsorption mechanism of  $\text{Pb}^{2+}$  on Bio-NiO could be electrostatic.

### 3.2.2. Effects of adsorbent dose

The amount of adsorbent is one of appropriate parameter which results the percentage removal of  $\text{Pb}^{2+}$  metal ion from water. By

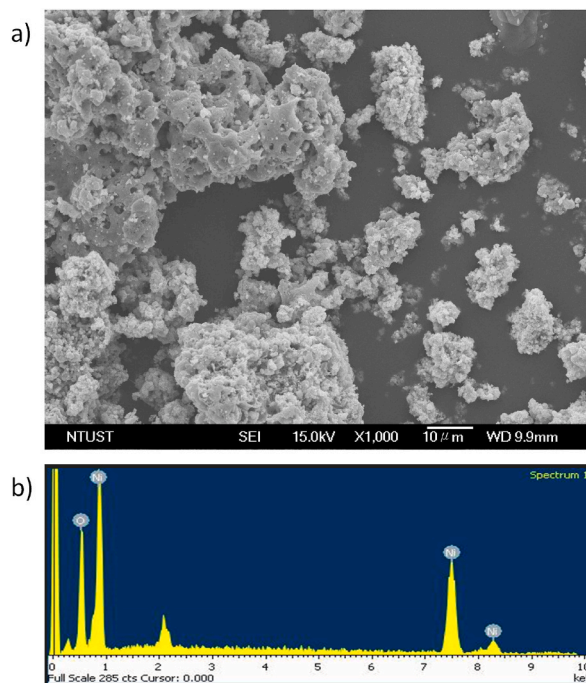


Fig. 3. SEM images for (a) Bio-NiO and (b) EDX for Bio-NiO NPs.

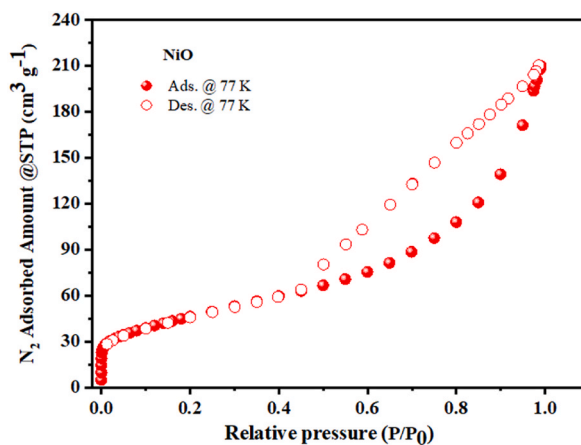
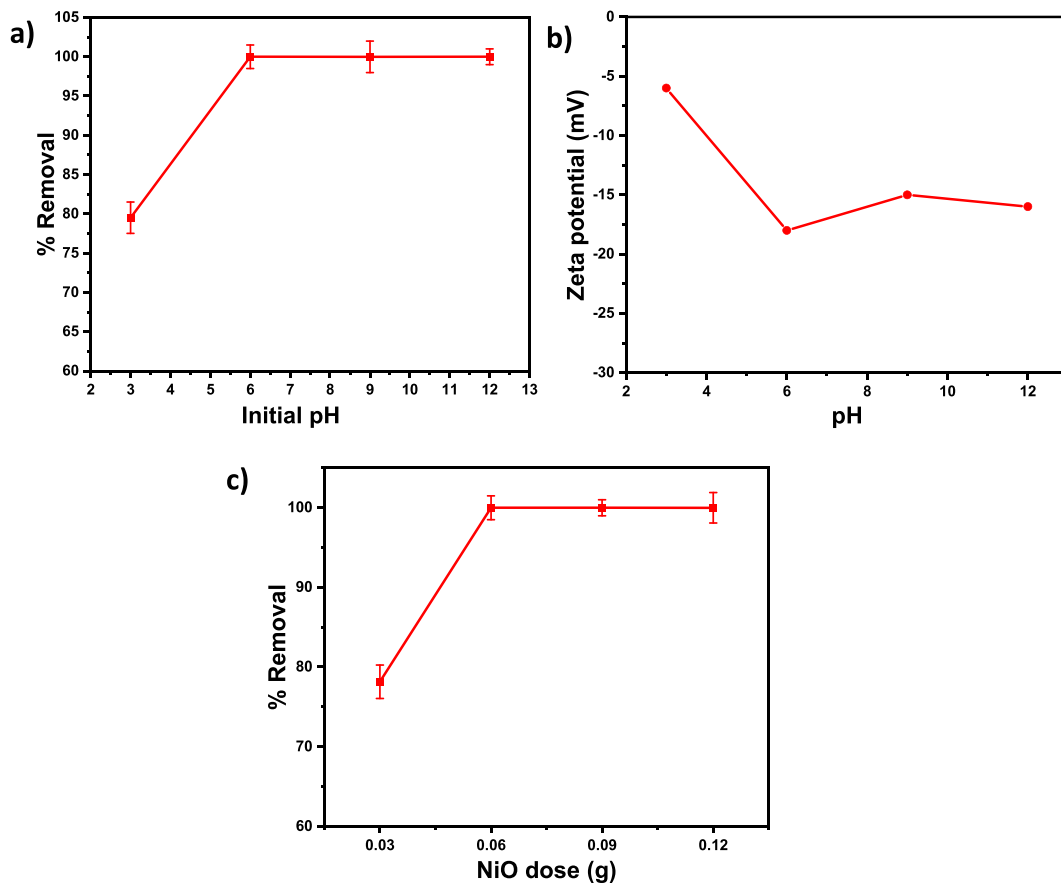


Fig. 4. Nitrogen adsorption-desorption isotherm for Bio-NiO NPs.

varying the amount of Bio-NiO NPs from 0.03 to 0.12 g, other parameters kept constant i.e. pH 6.0 (optimized from pH),  $\text{Pb}^{2+}$  concentration  $60 \text{ mgL}^{-1}$  and contact time 80 min, the percent removal was calculated. As indicated in Fig. 5c at dose of Bio-NiO NPs 0.03, 0.06, 0.09, and 0.12 g percentage removal was 78.15%, 99.99%, 99.99%, and 99.98%, respectively. The rise in percentage removal demonstrates the features of increased surface area, which leads to an increase in the number of vacant sites accessible for adsorption, but increasing the dose of adsorbent does not result in a greater percentage removal. This action in adsorption could be attributed to the enrichment of adsorption sites as a result of types of occurrence between adsorbed particles such as aggregation, which rises the dispersion path distance and leads to a decrease in sorption [43,44].

### 3.2.3. The effect of contact time

The effect of contact time on  $\text{Pb}^{2+}$  adsorption on Bio-NiO NPs was examined in the range of 40–100 min and shaken at 200 rpm at room temperature ( $297 \pm 2 \text{ K}$ ). Other parameters were constant (pH 6.0, NiO dose 0.06 g, initial  $\text{Pb}^{2+}$  ion concentration  $60 \text{ mgL}^{-1}$ ). As the reaction time increased until equilibrium was reached the removal of  $\text{Pb}^{2+}$  increased (Fig. 6a). No significant change in adsorption efficiency was seen after attaining equilibrium at 80 min, and this could be due to the saturation of active sites on the surface of the adsorbent, which causes this phenomenon [45]. However, the rate of percentage removal was slightly decreased after equilibrium



**Fig. 5.** a) Effects of initial pH ( $[Pb^{2+}] = 60 \text{ mg L}^{-1}$ , Bio-NiO NPs = 0.06 g, contact time = 80 min) b) Zeta potential Vs pH of Bio-NiO NPs c) Effect of Bio-NiO dose ( $[Pb^{2+}] = 60 \text{ mg L}^{-1}$ , pH = 6, contact time = 80 min).

time. From the result, the maximum percentage adsorption reached at 78.2% at 80 min and therefore, this contact time was selected for next following studies.

### 3.2.4. Effect of initial metal ion concentration

The adsorption of Pb<sup>2+</sup> by Bio-NiO NPs was tested by varying the Pb<sup>2+</sup> ion concentration from 40 to 100 mg L<sup>-1</sup> at ambient temperature, by maintaining all other conditions constant, i.e. from the previous experiment optimum pH 6.0, adsorbent dosage 0.06

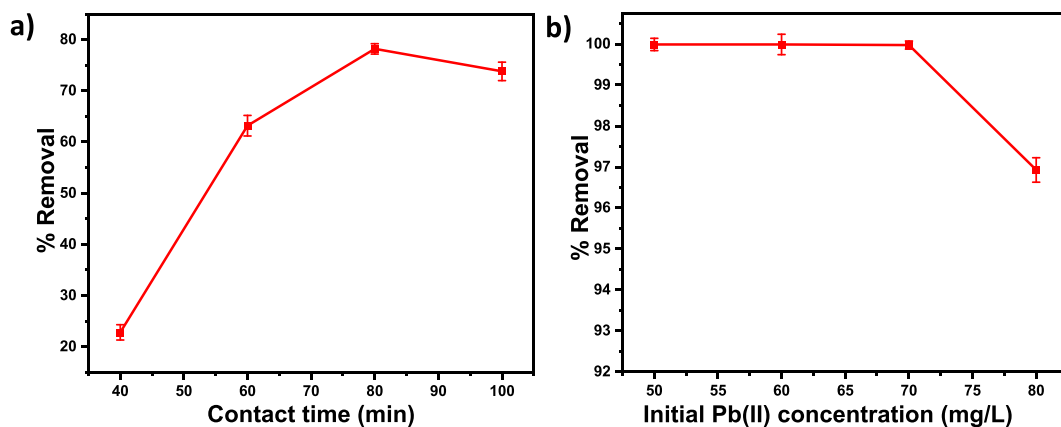


**Fig. 6.** Effects of a) contact time ( $[Pb^{2+}] = 60 \text{ mg L}^{-1}$ , Bio-NiO NPs = 0.06 g, pH = 6) and b) initial Pb<sup>2+</sup> ion (pH = 6, Bio-NiO NPs = 0.06 g, contact time = 80 min) on percentage removal of Pb<sup>2+</sup> by Bio-NiO NPs.

g, and contact time of 80 min. The dependence of the removal efficiency of Bio-NiO NPs on the equilibrium amounts of  $Pb^{2+}$  is displayed in Fig. 6b and maximum removal efficiency was 99.99% at  $60 \text{ mg L}^{-1}$ . However, with increasing amounts, significant numbers of  $Pb^{2+}$  ions are detected at the solid surface, and the number of sites becomes restricted lowering the percentage of adsorption [43, 46]. This suggests that the adsorption of  $Pb^{2+}$  depends on amounts of initial metal ion concentration. The maximum removal efficiency was recorded at a concentration of  $60 \text{ mg L}^{-1}$   $Pb^{2+}$  ion initial concentration. After evaluating the performance of Bio-NiO NPs towards on removal of  $Pb^{2+}$  we have compared its efficiency with other reported adsorbents which could be useful for the same applications. The comparisons showing for selected adsorbents is summarized in Table 1. With a pronounced adsorption efficiency, easy synthesis protocols, higher surface area, cost effective and user friendly, Bio-NiO NPs could meet the best adsorbent materials. In general, Bio-NiO NPs showed higher removal efficiencies for removal of  $Pb^{2+}$  from aqueous solutions better than the reported adsorbent materials.

### 3.3. Adsorption kinetics

Adsorption kinetics can be used to examine the adsorption mechanism as well as predict the stages that regulate the rate of adsorption. Furthermore, the optimal parameters for the metal ion removal process are determined using data from kinetic studies [52]. Pseudo-first-order kinetics is a kinetics model that explicitly governs physical adsorption based on the weak contact between the adsorbate and the adsorbent. The chemical interaction and adsorption processes, in contrast, are governed by the pseudo-second-order kinetic model. Pseudo-first order and second-order kinetics were used to examine the kinetics as calculated using Equations (4) and (5), respectively.

$$\log(q_e - q_t) = \log q_e - k_1/2.303 t \quad (4)$$

$$t/q_t = 1/k_2 q_e^2 e + 1/q_e t \quad (5)$$

Where  $q_t$  and  $q_e$  (mg/g) are the values of absorbed  $Pb^{2+}$  at  $t$  and equilibrium, respectively.  $k_1$  (1/min) and  $k_2$  (g/(mg·min)) are the rate constants of the first-order and second-order models, respectively.

The removal performance was performed at different contact time (40, 60, 80, 100 min) with initial concentrations of  $Pb^{2+}$   $60 \text{ mg L}^{-1}$  for kinetic study. The equilibrium is reached after 80 min as indicated in Fig. 6a. The kinetics of  $Pb^{2+}$  ion adsorption on Bio-NiO NPs were investigated, and the experimental results were used to calculate pseudo-first and second order parameters. Table 2 and Fig. 7 a and b describe the findings. Fig. 7b shows that the adsorption process was best matched with a pseudo-second order kinetic model and a correlation coefficient ( $R^2 = 0.99$ ), and the estimated  $q_e$  value is in good agreement with the experimental acquired value (Table 2).

### 3.4. Adsorption isotherms

An adsorption isotherm was operated to describe the equilibrium relationship between the adsorbate concentration in the liquid phase and the one on the solid surface of the adsorbent under the supplied conditions [53]. To demonstrate the mechanism of adsorption the most commonly employed Langmuir and Freundlich isotherms were applied. The Langmuir adsorption model implies monolayer adsorption onto a surface containing a finite number of homogeneous adsorption sites of adsorbent and, the adsorption equilibrium stated using the Langmuir equation (Equations (6) and (7)) [54,55].

$$\frac{1}{q_e} = \left( \frac{1}{c_e k_L q_m} \right) + \frac{1}{q_m} \quad (6)$$

Where  $q_m$  is maximum monolayer adsorption capacity (mg/g),  $k_L$  is the Langmuir constant, which is associated to the energy of adsorption (L/g),  $q_e$  and  $c_e$  are the adsorption capacity (mg/g) and equilibrium concentration ( $\text{mg L}^{-1}$ ), respectively. Plotting  $\frac{1}{q_e}$  versus  $\frac{1}{c_e}$  from the above equation results in a straight line of slope  $\frac{1}{q_m}$  and intercepts  $\frac{1}{k_L q_m}$ . The  $R_L$  value indicates the favorability of the isotherm, and it should be less than one for fitness.

**Table 1**  
Comparison of  $Pb^{2+}$  removal efficiency of Bio-NiO NPs with reported adsorbents.

Adsorbent	Dose	Time (min)	Removal efficiency (%)	Reference
PAMAM/TiO <sub>2</sub>	0.6 g	60	99.90	[47]
Alg@MgS	20 mg	60	91.00	[48]
PG-NiO	40 mg	60	99.00	[49]
DQ@Fe <sub>3</sub> O <sub>4</sub>	2.8 g	140	95.20	[50]
GO@TiO <sub>2</sub>	0.15 g	60	79.54	[51]
Bio-NiO	0.06 g	80	99.99	This work

Poly-amidoamine dendrimer (PAMAM), Alginate (Alg), Psidium guajava (PG), Dolomite-quartz (DQ), Graphene oxide (GO).

**Table 2**  
Kinetic parameters for the removal of Pb<sup>2+</sup> using Bio-NiO NPs.

Pseudo-first order	$q_e$ exp (mg/g)	$q_e$ cal (mg/g)	$K_1$	$R^2$
Pseudo-second order	59.62	6.72	-0.000013	0.89
	$q_e$ exp (mg/g)	$q_e$ cal (mg/g)	$K_2$	$R^2$
	59.62	60.13	79157.01	0.99

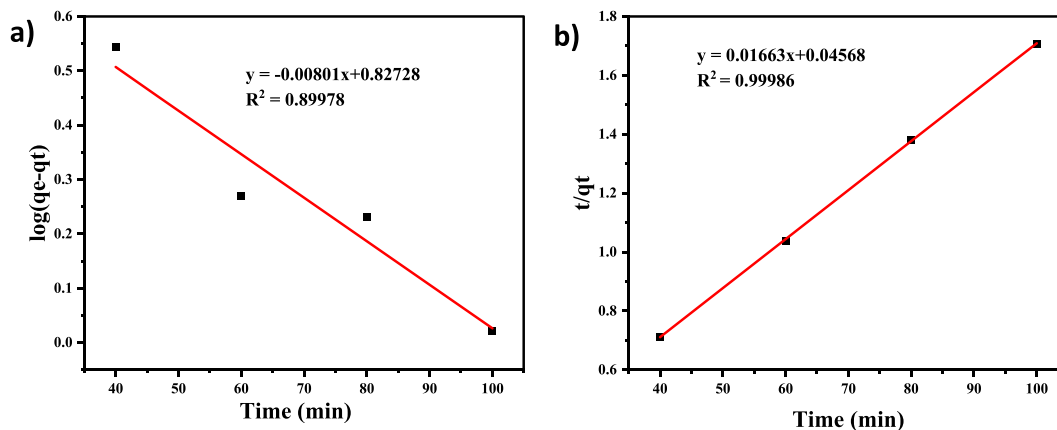


Fig. 7. a) Pseudo-first order kinetics and b) Pseudo-second order kinetics of Bio-NiO NPs for adsorption of Pb<sup>2+</sup>.

$$R_L = \frac{1}{1 + K_L C_o} \quad (7)$$

Where  $C_o$ , is the initial concentration of metal ion.

Freundlich adsorption isotherm is used for multilayer adsorption and heterogeneous surface, and it can be expressed by equation (Equation (8)) [56].

$$\log q_e = \log K_f + \frac{1}{n} \log c_e \quad (8)$$

Where  $K_f$  shows the Freundlich isotherm capacity (mg/g), and  $n$  denotes the adsorption intensity. A straight line with a slope  $K_f$  and intercept  $1/n$  is obtained by plotting  $\log q_e$  vs  $\log c_e$ . The value of  $n$  determines whether the adsorption is physical or chemical. The slope  $1/n$ , which ranges from 0 to 1, measures surface heterogeneity or adsorption intensity. As the value approaches zero, it becomes more heterogeneous [57].

The obtained results from isotherm models presented in Table 3 and Fig. 8 The parameters and correlation coefficients ( $R^2$ ) were suggests the adsorption process through the Freundlich isotherm model, indicating that the adsorption is chemical on heterogeneous surface of Bio-NiO NPs. From this study, the value of  $1/n < 1$  suggests, that the adsorption of Pb<sup>2+</sup> ion on the Bio-NiO NPs is favorable [55] and the highest adsorption capacity ( $q_e$ ) was found to be 60.13 mg/g.

### 3.5. Recovery studies

Regeneration of adsorbents is a crucial factor to consider when assessing an adsorbent's effectiveness from an economic, environmental, and practical standpoint. Regeneration involves recycling or recovering used adsorbents through cost-effective ways [58]. In this work, the addition of HCl and NaOH to the solution altered its pH, which in turn affected the recovery of the adsorbent (Bio-NiO NPs). In the typical experiments the recycling was performed by adding 0.015 M HCl eluent to the solution [59]. Initially, Pb<sup>2+</sup> was adsorbed on Bio-NiO NPs from 60 mL solutions at pH 6 that contained 100 mg L<sup>-1</sup> Pb<sup>2+</sup>. Then, for 45 min at 25 °C, Bio-NiO NPs were stripped using 25 mL of eluent string. After separating the Bio-NiO NPs, the supernatant was examined. The adsorption-desorption cycles were carried out five times for every analysis. The results indicated that the first, second, third, fourth, and fifth cycles, respectively, produced removal rates of 99, 98, 95.4, 92.6, and 90.8% (Fig. 9). The outcomes showed that, across a five-cycle study, Bio-NiO NPs exhibit good stability and recovery.

## 4. Conclusions

NiO NPs was successfully created using *Hagenia abyssinica* plant extract as a template and reducing agent through greener co-precipitation approach. The phase, shape, and surface groups were investigated using XRD, SEM/EDX, and FT-IR, respectively. At

**Table 3**  
Parameters for Isotherm studies of removal of  $Pb^{2+}$  using Bio-NiO NPs.

Langmuir constants				Freundlich constants			
Parameter	$q_m$ (mg/g)	$K_L$ (L/mg)	$R_L$	$R^2$	$1/n$	$K_F$	$R^2$
	6.71	0.20	13.02	0.97	0.47	0.00046	0.99

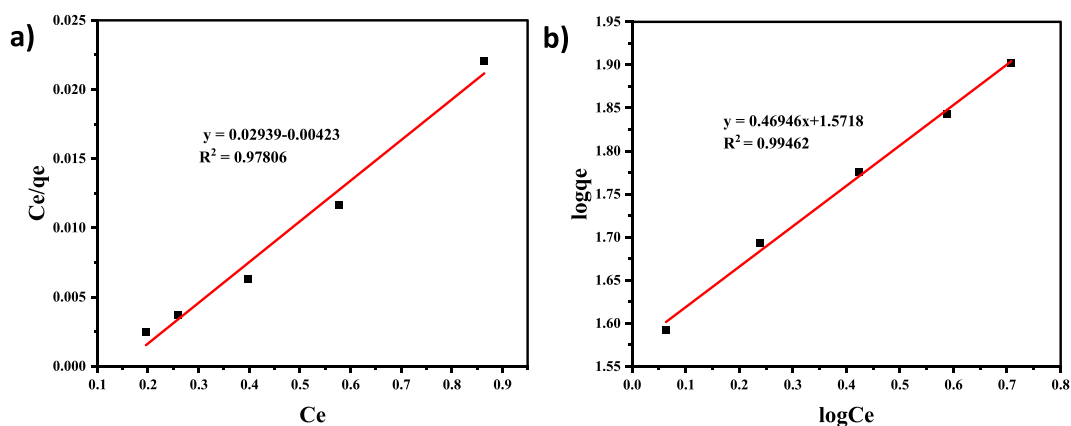


**Fig. 8.** a) Langmuir isotherm and b) Freundlich isotherm for Bio-NiO for removal of  $Pb^{2+}$ .

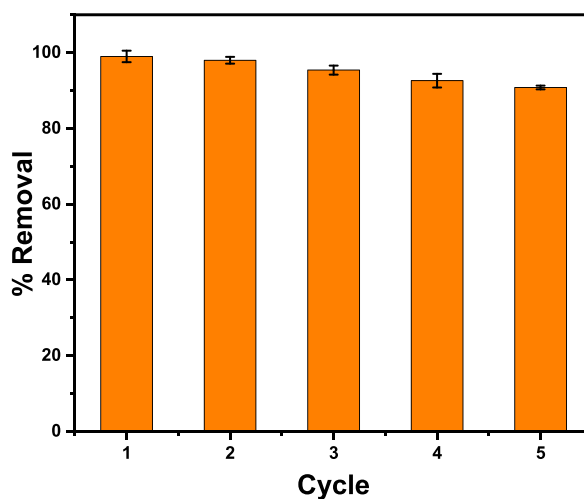


**Fig. 9.** Reusability studies of Bio-NiO NPs on the removal of  $Pb^{2+}$  for consecutive five cycles.

77 K,  $N_2$  adsorption-desorption isotherms were collected to investigate porosity attributes such as surface area, pore size distribution, and pore volume. The resulting Bio-NiO NPs exhibits a mesoporous structure and a high surface area. The results showed that the adsorption capabilities of Bio-NiO NPs were explored using various factors such as solution pH, Bio-NiO dose, contact time, and  $Pb^{2+}$  concentrations. Bio-NiO NPs showed a remarkable adsorption performance in aqueous solutions (99.99 % sorption of  $Pb^{2+}$ ). Moreover, the adsorption kinetics process was driven by pseudo-second-order kinetics, and an adsorption isotherm was fitted with Freundlich isotherm, confirming that the multilayer adsorption of  $Pb^{2+}$  ions onto Bio-NiO NPs adsorbent occurs via a chemical interaction. Therefore, the synthesized Bio-NiO NPs could be cost effective, user friendly and potential candidate for adsorptive elimination of heavy metals from contaminated water.

#### Funding statement

This work was supported by Wollo University.

## Data availability statement

The data that has been used is confidential.

## Additional information

No additional information is available for this paper.

## CRediT authorship contribution statement

**Abdurohman Eshtu Ferenji:** Writing – original draft, Methodology, Investigation. **Yeshi Endris Hassen:** Writing – original draft, Methodology, Data curation. **Shewaye Lakew Mekuria:** Writing – review & editing, Validation, Formal analysis. **Wubshet Mekonnen Girma:** Writing – review & editing, Supervision, Resources, Funding acquisition, Formal analysis, Conceptualization.

## Declaration of competing interest

The authors declare that they have no known competing financial interests or personal relationships that could have appeared to influence the work reported in this paper.

## Acknowledgements

The authors would like to thank Wollo University for financial support through graduate student program. The author also would like to gratefully acknowledge National Taiwan Science and Technology University for SEM/EDX imaging and Adama Science and Technology University for XRD analysis.

## References

- [1] H. Ali, E.I. Khan, I. Environmental chemistry and ecotoxicology of hazardous heavy metals: environmental persistence, toxicity, and bioaccumulation, *J. Chem.* 2019 (2019) 1–14.
- [2] J. Wu, M. Yan, S. Lv, W. Yin, H. Bu, L. Liu, P. Li, H. Deng, X. Zheng, Preparation of highly dispersive and antioxidative nano zero-valent iron for the removal of hexavalent chromium, *Chemosphere* 262 (2021) 127733.
- [3] E. Mahmoudi, S. Azizkhani, A.W. Mohammad, L.Y. Ng, A. Benamor, W.L. Ang, M. Ba-Abbad, Simultaneous removal of Congo red and cadmium (II) from aqueous solutions using graphene oxide–silica composite as a multifunctional adsorbent, *J. Environ. Sci.* 98 (2020) 151–160.
- [4] P.B. Tchounwou, C.G. Yedjou, A.K. Patlolla, D.J. Sutton, Heavy metal toxicity and the environment, *Exp Suppl* 101 (2012) 133–164.
- [5] R. Singh, R. Bhatia, Optimization and experimental design of the Pb<sup>2+</sup> adsorption process on a nano-Fe<sub>3</sub>O<sub>4</sub>-based adsorbent using the response surface methodology, *ACS Omega* 5 (43) (2020) 28305–28318.
- [6] B. Lam, S. Déon, N. Morin-Crini, G. Crini, P. Fievet, Polymer-enhanced ultrafiltration for heavy metal removal: influence of chitosan and carboxymethyl cellulose on filtration performances, *J. Clean. Prod.* 171 (2018) 927–933.
- [7] B. Dhir, Potential of biological materials for removing heavy metals from wastewater, *Environ. Sci. Pollut. Res. Int.* 21 (3) (2014) 1614–1627.
- [8] T. Kameda, Y. Suzuki, T. Yoshioka, Removal of arsenic from an aqueous solution by coprecipitation with manganese oxide, *J. Environ. Chem. Eng.* 2 (4) (2014) 2045–2049.
- [9] P.V. Nidheesh, T.S.A. Singh, Arsenic removal by electrocoagulation process: recent trends and removal mechanism, *Chemosphere* 181 (2017) 418–432.
- [10] A. Abejón, A. Garea, A. Irabien, Arsenic removal from drinking water by reverse osmosis: minimization of costs and energy consumption, *Separ. Purif. Technol.* 144 (2015) 46–53.
- [11] A.F.T. El-Din, M.E. El-Khouly, E.A. Elshehy, A.A. Atia, W.A. El-Said, Cellulose acetate assisted synthesis of worm-shaped mesopores of MgP ion-exchanger for cesium ions removal from seawater, *Microporous Mesoporous Mater.* 265 (2018) 211–218.
- [12] M.Z. Bani-Fwaz, A.A. El-Zahhar, H.S.M. Abd-Rabboh, M.S. Hamdy, M. Shkir, Synthesis of NiO nanoparticles by thermal routes for adsorptive removal of crystal violet dye from aqueous solutions, *Int. J. Environ. Anal. Chem.* 101 (8) (2019) 1126–1144.
- [13] I.H. Ali, M.Z. Bani-Fwaz, A.A. El-Zahhar, R. Marzouki, M. Jemmali, S.M. Ebraheem, Gum Arabic-magnetite nanocomposite as an eco-friendly adsorbent for removal of lead(II) ions from aqueous solutions: equilibrium, kinetic and thermodynamic studies, *Separations* 8 (11) (2021) 224.
- [14] M. Barakat, New trends in removing heavy metals from industrial wastewater, *Arab. J. Chem.* 4 (4) (2011) 361–377.
- [15] J. Tian, P. Tian, G. Ning, H. Pang, Q. Song, H. Cheng, H. Fang, Synthesis of porous MgAl<sub>2</sub>O<sub>4</sub> spinel and its superior performance for organic dye adsorption, *RSC Adv* 5 (2015) 5123–5130.
- [16] A.M. Mahmoud, F.A. Ibrahim, S.A. Shaban, N.A. Youssef, Adsorption of heavy metal ion from aqueous solution by nickel oxide nano catalyst prepared by different methods, *Egyptian Journal of Petroleum* 24 (1) (2015) 27–35.
- [17] M. Yimer, S.N. Ansari, B.A. Berehe, K.K. Gudimella, G. Gedda, W.M. Girma, N. Hasan, S. Tasneem, Adsorptive removal of heavy metals from wastewater using Cobalt-diphenylamine (Co-DPA) complex, *BMC Chem* 18 (1) (2024) 23.
- [18] S.M. Khalith, R.R. Anirud, R. Ramalingam, S.K. Karuppanan, M.J.H. Dowlath, K. Pandion, B. Ravindran, S. WoongChang, D. Ovi, M.V. Arasu, Synthesis and characterization of magnetite carbon nanocomposite from agro waste as chromium adsorbent for effluent treatment, *Environ. Res.* 202 (2021) 111669.
- [19] N.M. Hosny, Synthesis, characterization and optical band gap of NiO nanoparticles derived from anthranilic acid precursors via a thermal decomposition route, *Polyhedron* 30 (3) (2011) 470–476.
- [20] T. Mahmood, M. Saddique, A. Naeem, S. Mustafa, J. Hussain, B. Dilara, Cation exchange removal of Zn from aqueous solution by NiO, *J. Non-Cryst. Solids* 357 (3) (2011) 1016–1020.
- [21] S. Prabhu, T.D. Thangadurai, P.V. Bharathy, P. Kalugasalam, Synthesis and characterization of nickel oxide nanoparticles using Clitoria ternatea flower extract: photocatalytic dye degradation under sunlight and antibacterial activity applications, *Results in Chemistry* 4 (2022) 100285.
- [22] T. Ali, M.F. Warsi, S. Zulfiqar, A. Sami, S. Ullah, A. Rasheed, I.A. Alsafari, P.O. Agboola, I. Shakir, M.M. Baig, Green nickel/nickel oxide nanoparticles for prospective antibacterial and environmental remediation applications, *Ceram. Int.* 48 (6) (2022) 8331–8340.
- [23] R. Ramalingam, M.H.U.T. Fazil, N.K. Verma, K.D. Arunachalam, Green synthesis, characterization and antibacterial evaluation of electrospun nickel oxide nanofibers, *Mater. Lett.* 256 (2019) 126616.
- [24] B.Y. Hussein, A.M. Mohammed, Biosynthesis and characterization of nickel oxide nanoparticles by using aqueous grape extract and evaluation of their biological applications, *Results in Chemistry* 3 (2021) 100142.

- [25] U. Baig, M.K. Uddin, M. Gondal, Removal of hazardous azo dye from water using synthetic nano adsorbent: facile synthesis, characterization, adsorption, regeneration and design of experiments, *Colloids Surf. A Physicochem. Eng. Asp.* 584 (2020) 124031.
- [26] Z. Sabouri, A. Rangrazi, M.S. Amiri, M. Khatami, M. Darroudi, Green synthesis of nickel oxide nanoparticles using *Salvia hispanica* L. (chia) seeds extract and studies of their photocatalytic activity and cytotoxicity effects, *Bioproc. Biosyst. Eng.* 44 (11) (2021) 2407–2415.
- [27] S. Ghazal, N. Khandannasab, H.A. Hosseini, Z. Sabouri, A. Rangrazi, M. Darroudi, Green synthesis of copper-doped nickel oxide nanoparticles using okra plant extract for the evaluation of their cytotoxicity and photocatalytic properties, *Ceram. Int.* 47 (19) (2021) 27165–27176.
- [28] Z.T. Khodair, N.M. Ibrahim, T.J. Kadhim, A.M. Mohammad, Synthesis and characterization of nickel oxide (NiO) nanoparticles using an environmentally friendly method, and their biomedical applications, *Chem. Phys. Lett.* 797 (2022) 139564.
- [29] W.W. Melkamu, L.T. Bitew, Green synthesis of silver nanoparticles using *Hagenia abyssinica* (Bruce) JF Gmel plant leaf extract and their antibacterial and anti-oxidant activities, *Heliyon* 7 (11) (2021) e08459.
- [30] T. Wolde, B. Bizuayehu, T. Hailemariam, K. Tiruha, Phytochemical analysis and antimicrobial activity of *Hagenia abyssinica*, *Indian J. Pharm. Pharmacol.* 3 (3) (2016) 127–134.
- [31] H.A. Murthy, T.D. Zeleke, C. Ravikumar, M.A. Kumar, H. Nagaswarupa, Electrochemical properties of biogenic silver nanoparticles synthesized using *Hagenia abyssinica* (Bruce) JF. Gmel. medicinal plant leaf extract, *Mater. Res. Express* 7 (5) (2020), 055016-05530.
- [32] K. Lingaraju, H. Raja Naika, H. Nagabhushana, K. Jayanna, S. Devaraja, G. Nagaraju, Biosynthesis of Nickel oxide Nanoparticles from *Euphorbia heterophylla* (L.) and their biological application, *Arab. J. Chem.* 13 (3) (2020) 4712–4719.
- [33] U. Holzwarth, N. Gibson, The Scherrer equation versus the 'Debye-Scherrer equation', *Nat. Nanotechnol.* 6 (9) (2011) 534, 534.
- [34] S. Ananthi, M. Kavitha, A. Balamurugan, E. Ranjith Kumar, G. Magesh, A.F. Abd El-Rehim, C. Srinivas, P. Anilkumar, J. Suryakanth, C. Sharmila Rahale, Synthesis, analysis and characterization of camellia sinensis mediated synthesis of NiO nanoparticles for ethanol gas sensor applications, *Sensor. Actuator. B Chem.* 387 (2023) 133742.
- [35] W. Ahmad, S.C. Bhatt, N. Kaur, Plant extract mediated approach towards the synthesis of NiO nanoparticles: evaluation of its antibacterial, antioxidant and photocatalytic activity, *Vietnam Journal of Chemistry* 61 (4) (2023) 445–454.
- [36] A.M. Hamdan, A. Sardi, R.P. Reksamunandar, Z. Maulida, D.A. Arsa, S.S. Lubis, K. Nisah, Green synthesis of NiO nanoparticles using a Cd hyperaccumulator (*Lactuca sativa* L.) and its application as a Pb(II) and Cu(II) adsorbent, *Environ. Nanotechnol. Monit. Manag.* 21 (2024) 100910.
- [37] G. Murtaza, Z. Ahmed, M. Valipour, I. Ali, M. Usman, R. Iqbal, U. Zulfiqar, M. Rizwan, S. Mahmood, A. Ullah, M. Arslan, M.H.U. Rehman, A. Ditta, A. Tariq, Recent trends and economic significance of modified/functionalized biochars for remediation of environmental pollutants, *Sci. Rep.* 14 (1) (2024) 217.
- [38] M.A. Behnajady, S. Bimeghdar, Synthesis of mesoporous NiO nanoparticles and their application in the adsorption of Cr(VI), *Chem. Eng. J.* 239 (2014) 105–113.
- [39] G.H. Chala, T.D. Zeleke, Green synthesis of magnetite nanoparticles using *Catha edulis* plant leaf extract for removal of hexavalent Chromium from aqueous solution, *Int. J. Nano Dimens. (IJND)* 14 (1) (2023) 73–90.
- [40] H. Karami, Heavy metal removal from water by magnetite nanorods, *Chem. Eng. J.* 219 (2013) 209–216.
- [41] K.Y. Kumar, T.V. Raj, S. Archana, S.B. Prasad, S. Olivera, H. Muralidhara, SnO<sub>2</sub> nanoparticles as effective adsorbents for the removal of cadmium and lead from aqueous solution: adsorption mechanism and kinetic studies, *J. Water Proc. Eng.* 13 (2016) 44–52.
- [42] A.E. Ferenji, D.M. Kabtamu, A.H. Assen, G. Gedda, A.A. Muhabie, M. Berrada, W.M. Girma, *Hagenia abyssinica*-biomediated synthesis of a magnetic Fe(3)O(4)/NiO nanoadsorbent for adsorption of lead from wastewater, *ACS Omega* 9 (6) (2024) 6803–6814.
- [43] Y.E. Hassen, G. Gedda, A.H. Assen, D.M. Kabtamu, W.M. Girma, *Dodonaea angustifolia* extract-assisted green synthesis of the Cu(2)O/Al(2)O(3) nanocomposite for adsorption of Cd(II) from water, *ACS Omega* 8 (19) (2023) 17209–17219.
- [44] M.E. Bidhendi, E. Parandi, M.M. Meymand, H. Sereshti, H.R. Nodeh, S.-W. Joo, Y. Vasseghian, N.M. Khatir, S. Rezanian, Removal of lead ions from wastewater using magnesium sulfide nanoparticles caged alginate microbeads, *Environ. Res.* 216 (2023) 114416.
- [45] S.A. Haris, S. Dabagh, H. Mollasalehi, Y.N. Ertas, Alginate coated superparamagnetic iron oxide nanoparticles as nanocomposite adsorbents for arsenic removal from aqueous solutions, *Separ. Purif. Technol.* 310 (2023) 123193.
- [46] A. Alipour, S. Zarinabadi, A. Azimi, M. Mirzaei, Adsorptive removal of Pb(II) ions from aqueous solutions by thiourea-functionalized magnetic ZnO/nanocellulose composite: optimization by response surface methodology (RSM), *Int. J. Biol. Macromol.* 151 (2020) 124–135.
- [47] A. Maleki, B. Hayati, F. Najafi, F. Gharibi, S.W. Joo, Heavy metal adsorption from industrial wastewater by PAMAM/TiO<sub>2</sub> nanohybrid: preparation, characterization and adsorption studies, *J. Mol. Liq.* 224 (2016) 95–104.
- [48] M. Esmaili Bidhendi, E. Parandi, M. Mahmoudi Meymand, H. Sereshti, H. Rashidi Nodeh, S.W. Joo, Y. Vasseghian, N. Mahmoudi Khatir, S. Rezanian, Removal of lead ions from wastewater using magnesium sulfide nanoparticles caged alginate microbeads, *Environ. Res.* 216 (Pt 1) (2023) 114416.
- [49] D. Chukwu Onu, A. Kamoru Babayemi, T. Chinedu Egbosiuba, B. Onyinye Okafor, I. Jacinta Ani, S. Mustapha, J. Oladejo Tijani, W. Chukwuemeke Ulakpa, P. Eguono Ovuoraye, A. Saka Abdulkareem, Isotherm, kinetics, thermodynamics, recyclability and mechanism of ultrasonic assisted adsorption of methylene blue and lead (II) ions using green synthesized nickel oxide nanoparticles, *Environ. Nanotechnol. Monit. Manag.* 20 (2023) 100818.
- [50] A. El Mouden, N. El Messaoudi, A. El Guerraf, A. Bouich, V. Mehmeti, A. Lacherai, A. Jada, J.H. Pine Americo-Pinheiro, Removal of cadmium and lead ions from aqueous solutions by novel dolomite-quartz@Fe(3)O(4) nanocomposite fabricated as nanoadsorbent, *Environ. Res.* 225 (2023) 115606.
- [51] M.E.A. El-Aziz, A.M. Youssef, K.H. Kamal, I. Kelnar, S. Kamel, Preparation and performance of bionanocomposites based on grafted chitosan, GO and TiO(2)-NPs for removal of lead ions and basic-red 46, *Carbohydr. Polym.* 305 (2023) 120571.
- [52] M.A. Behnajady, S. Bimeghdar, Synthesis of mesoporous NiO nanoparticles and their application in the adsorption of Cr (VI), *Chem. Eng. J.* 239 (2014) 105–113.
- [53] M.R. Abukhadra, M.A. Sayed, A.M. Rabie, S.A. Ahmed, Surface decoration of diatomite by Ni/NiO nanoparticles as hybrid composite of enhanced adsorption properties for malachite green dye and hexavalent chromium, *Colloids Surf. A Physicochem. Eng. Asp.* 577 (2019) 583–593.
- [54] M.M. Majid, V. Kordzadeh-Kermani, V. Ghalandari, A. Askari, M. Sillanpää, Adsorption isotherm models: a comprehensive and systematic review (2010– 2020), *Sci. Total Environ.* 812 (2022) 151334.
- [55] Z.M. Khoshhesab, Z. Hooshyar, M. Sarfaraz, Removal of Pb (II) from aqueous solutions by NiO nanoparticles, synthesis and reactivity in inorganic, metal-organic, *Nano-Metal Chemistry* 41 (8) (2011) 1046–1051.
- [56] M. Safari, R. Rezaee, R.D.C. Soltani, E. Asgari, Dual immobilization of magnetite nanoparticles and biosilica within alginate matrix for the adsorption of Cd(II) from aquatic phase, *Sci. Rep.* 12 (1) (2022) 11473.
- [57] A. Kumar, S. Sidharth, B. Kandasubramanian, A review on algal biosorbents for heavy metal remediation with different adsorption isotherm models, *Environ. Sci. Pollut. Res. Int.* 30 (14) (2023) 39474–39493.
- [58] M. Vakili, S. Deng, G. Cagnetta, W. Wang, P. Meng, D. Liu, G. Yu, Regeneration of chitosan-based adsorbents used in heavy metal adsorption: a review, *Separ. Purif. Technol.* 224 (2019) 373–387.
- [59] S. Rajput, C.U. Pittman Jr., D. Mohan, Magnetic magnetite (Fe<sub>3</sub>O<sub>4</sub>) nanoparticle synthesis and applications for lead (Pb<sup>2+</sup>) and chromium (Cr<sup>6+</sup>) removal from water, *J. Colloid Interface Sci.* 468 (2016) 334–346.